Journal of South American Earth Sciences 105 (2021) 102956

Contents lists available at ScienceDirect

Journal of South American Earth Sciences

journal homepage: www.elsevier.com/locate/jsames

Triassic-Jurassic thermal evolution and exhumation of the western Gondwana foreland: Thermochronology and basalt thermobarometry from the Argentine Sierras Pampeanas

Federico Martina [a,*], Pilar Ávila [a], Federico M. Dávila [a], Mauricio Parra [b]

[a] CICTERRA (CONICET - UNC), Córdoba, Argentina
[b] Instituto de Energia e Ambiente, Universidad de Sao Paulo, Brazil

ARTICLE INFO

Keywords:
Apatite fission track modelling
Whole-rock geochemistry
Mesozoic
Geodynamics
Unconformity formation

ABSTRACT

The geological record of the eastern Sierras Pampeanas province, in the modern Andean broken foreland of Argentina can be divided into four main events: (1) Proterozoic to early Paleozoic collisional tectonics, (2) middle-late Paleozoic anorogenic magmatism, relief generation and glacial paleovalley formation followed by (3) a classical foreland filling in the Permian and two proximal alluvial sedimentation associated with (3) Cretaceous rifting and (4) Neogene intermontane foreland accumulation. The region lacks Silurian, Triassic and Jurassic records, commonly associated with unknown deformation and/or no-sedimentation stages (bypass zone?). In this work, we analyzed the Mesozoic (Triassic-Jurassic) Pampean unconformity, using low-temperature thermochronological modelling. After a rapid Carboniferous cooling track, a Triassic reheating followed by a slow Jurassic to Cretaceous cooling. Considering that (1) no Triassic basins have been described to date in the eastern Sierras Pampeanas (i.e., reheating cannot be related to burial), (2) coeval surface heat flows are anomalously high in western Sierras Pampeanas, in the Ischigualasto basin, and (3) our petrogenetic modelling on Triassic basalts evidence mantle potential temperatures of ~1350–1400 °C (i.e., the heat source cannot be related with an anomalously high basal heat flows and/or mantle plumes); we interpreted the formation of the Mesozoic unconformity as a result of ridge collision and slab window formation, followed by slab rollback. Both processes might have affected not only the surface heat flow but also triggered a lithospheric thickness reduction, which drove isostatic rebound. In this context, the Jurassic history of the unconformity could be associated with cooling by erosion and exhumation until the Cretaceous, when the region was under extension. Our model agrees with other observations like the formation of back-arc hydrocarbon-productive Triassic-Jurassic depocenters to the west (Cuyo and Ischigualasto basins) and the magmatic evolution, from 28° to 34° SL, described along the Chilean margin.

1. Introduction

The pre-Andean geologic and tectonic history across the foreland areas of western Gondwana, particularly in the eastern Sierras Pampeanas (Sierras de Córdoba in west-central Argentina), can be summarized in three major stages: (1) an early-middle Paleozoic stage, when the area was under sea level and faced subduction and/or terranes collisions towards west (see Ramos, 2009, among others), followed by (2) a middle-late Paleozoic stage with a long erosional/no-depositional period interrupted by localized glacial paleovalley formation (Astini and Del Papa, 2014), and crowned by (3) a Cretaceous stage associated with rifting, dominated by continental alluvial sedimentation (Schmidt et al., 1995). No Triassic and Jurassic records have been reported across this region. However, localized and deep hydrocarbon-productive rift basins with basalts developed ~200 km to the west (between the Cordillera Frontal and western Sierras Pampeanas, from 28° to 40° SL) during this lap time. From these pre-Andean stratigraphic relationships, a question arises: what does this major discordance between basement/Upper Paleozoic and Upper Cretaceous across the eastern Sierras Pampeanas represent? Although, during this long time period (~140 my) no sedimentary records have been reported in this distal regions, it is possible to study this major discordance using reported low-temperature thermochronology ages (see Jordan et al., 1989; Löbens et al., 2011a,b, 2013; Dávila and Carter, 2013; Bense et al., 2013, Richardson et al., 2013;

* Corresponding author.
E-mail address: fmartina@unc.edu.ar (F. Martina).

https://doi.org/10.1016/j.jsames.2020.102956
Received 18 July 2020; Received in revised form 9 October 2020; Accepted 9 October 2020
Available online 20 October 2020

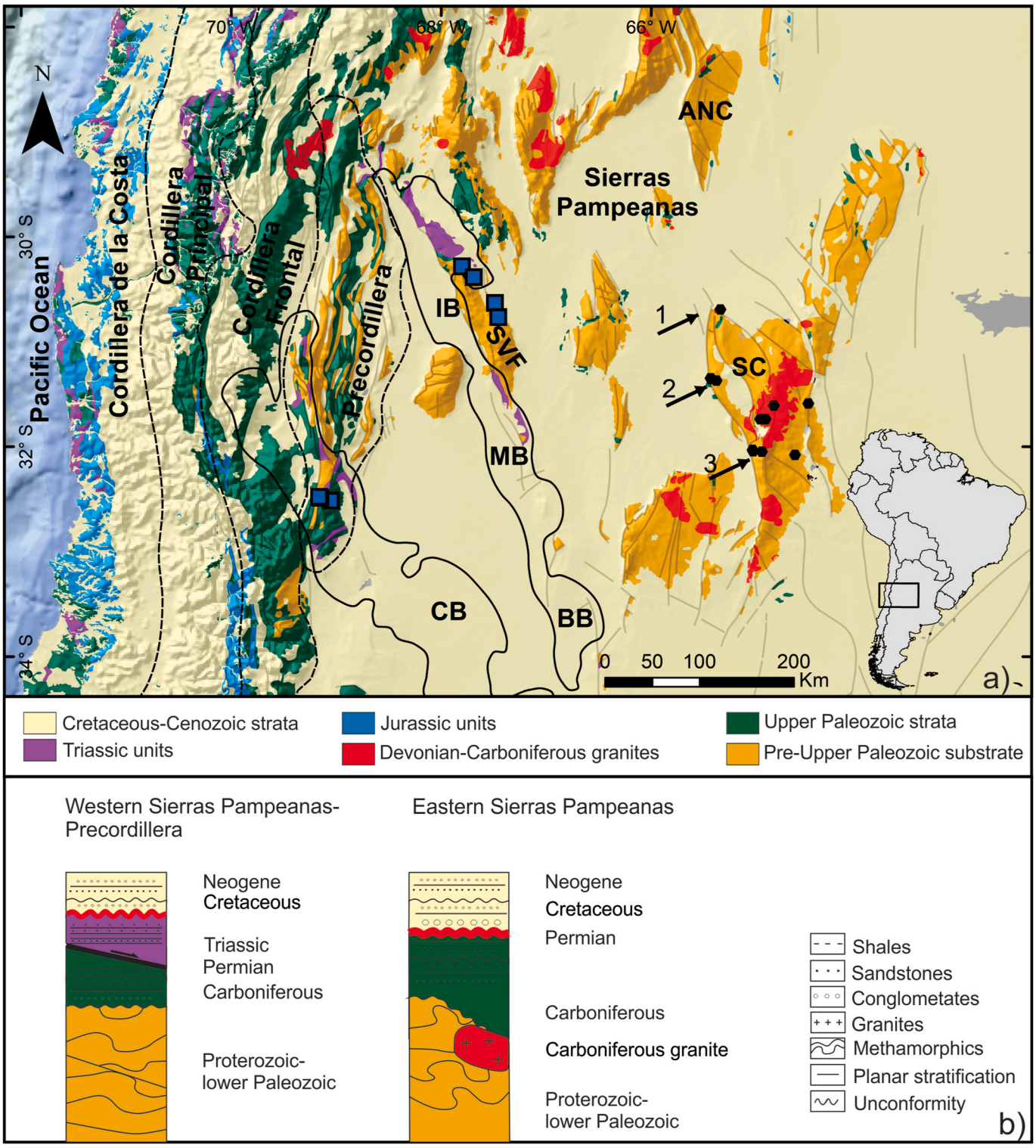

Fig. 1. (a) Map of the south Central Andes, between central Argentina and the Chilean trench in the Pacific Ocean, depicting the main geological provinces (Sierras Pampeanas broken foreland and Cordilleran belts; black dashed lines). Arrows 1 (Serrezuela range), 2 (Pocho range) and 3 (Yacanto) indicate locations of resampled thermochronological data from Dávila et al. (submitted). Black solid lines show the location of the Triassic basins: IB-Ischigualasto basin; MB-Marayes basin; BB-Beazley basin; CB-Cuyo basin. Blue squares indicate geochemical sample locations. Black hexagons show the location of thermocronological samples in the Sierras de Córdoba (SC). SVF-Sierra de Valle Fértil; ANC-Sierras de Ancasti. (b) Synthetic stratigraphy from west to east and unit correlations across strike. Red line shows the major unconformity analyzed in this work. (For interpretation of the references to colour in this figure legend, the reader is referred to the Web version of this article.)

Dávila et al., submitted). These data not only allow evidencing the exhumation history of the Gondwanaland foreland, but also the thermal evolution of the paleo-lithosphere in order to evaluate different geodynamic scenarios.

In this work, we resampled reported low-temperature thermochronology from the easternmost Sierras Pampeanas (Löbens et al., 2011a,b, 2017; Bense et al., 2013; Dávila et al., submitted), in the westernmost Sierras de Córdoba. The analyzed samples come from basement rocks, (a) an Early Carboniferous granite, which is covered by upper Carboniferous and lower Permian strata, and (b) two different spots southward, on Proterozoic-Paleozoic basement (Pocho and Yacanto areas). These data allowed us to remodel the thermal evolution of the easternmost Sierras Pampeanas using different geological constraints. We compared our results with forward thermochronological models (>300 ages) carried out in other parts of the Sierras Pampeanas (see Dávila and Carter, 2013). In addition, we supported our analysis with a preliminary thermobarometric modeling of poorly fractionated Triassic basalts. These basalts are located immediately to the west of the Sierra de Córdoba, in the western Sierras Pampeanas and Precordillera. We used these records since there are not enough geochemical data of Triassic-Jurassic basalts in the eastern Sierras Pampeanas. This thermobarometric model enabled us to improve our thermochronological analysis as well as determine the Mesozoic ambient mantle temperature for the whole Sierras Pampeanas.

2. Geological setting

The study area is located in the foreland of western Gondwana, in the Sierras Pampeanas province (32.5°-30° SL, see Fig. 1a). Between the Triassic and Jurassic, this region would have only accommodated stratigraphic records toward the west and along the Cordilleran belts (see Fig. 1a). The most known Triassic rift depocenters (see Fig. 1a) are Ischigualasto, Marayes, Beazley and Cuyo basins (see Ramos and Kay, 1991), covering part of the westernmost Sierras Pampeanas, Precordillera and Cordillera Frontal, in western Argentina (Fig. 1a). These basins are typical continental taphrogenic depocenters, 1000 s m thick, showing a fining-thinning upward arrangement (Ávila et al., 2006). Diagnostic alkaline basalts, interlayered with the sedimentary successions, conducted different studies (e.g., Ramos and Kay, 1991; Orellano et al., 2019) to interpret an extensional tectonic scenario. We provided a new geochemical data from a basalt sample from the Cuyo basin (see details in Table SM3). In this region, no Jurassic records have been reported, with the exception of a very thin and extremely localized section in the Mogna anticline core (Fig. 1a), in the western Sierras Pampeanas (Martí nez and Colombi, 2011). At these latitudes, Jurassic only crops out from the main Cordillera to the west in Chile (Mpodozis and Ramos, 2008). During the Triassic and Jurassic, like the western rest margin of Gondwana, the study region was affected by subduction (Ramos, 2009) and occupied a pericratonic or distal foreland belt, at >600 km from the contemporaneous accretionary prism (see Hyppolito et al., 2015). The lack of records during the Triassic and Jurassic in most of the Sierras Pampeanas, particularly the central and eastern areas, would have resulted in the development of a lengthy unconformity (Pampean unconformity from now), poorly analyzed in the literature.

To analyze the Pampean unconformity, we focused our thermochronological modelling along the westernmost Sierras de Córdoba (Pocho-Serrezuela ranges, see Fig. 1a), in the eastern Sierras Pampeanas. We chose this area because the western Sierras Pampeanas, in contrast, was affected by deep burial (Triassic rift basins) and consequently, the thermal history might have been masked by the subsidence and sediment accumulation. In this region, Proterozoic to lower Paleozoic crystalline basement crops out as well as Late Paleozoic to Cenozoic strata, with a long stratigraphic gap between the Upper Permian and late Lower Cretaceous (Gordillo and Lencinas, 1979). These unit relationships allowed us to analyze the Mesozoic exhumation history in the area. The stratigraphic column is relatively simple (Fig. 1b): (i) a Proterozoic-Lower Paleozoic metamorphic complex (low to high grade) (ii) intruded by lower to upper Paleozoic granitoids, which are both covered by (iii) Upper Paleozoic continental sedimentary successions. A (iv) major discordance separates these units from (v) rift-related Cretaceous and synorogenic Neogene strata. The stratigraphic thickness of these units ranges from tens to a few hundreds of meters.

The northernmost apatite fission track (AFT) sample along the western Sierras de Cordoba derives from an Early Carboniferous granite (Serrezuela pluton, Gómez, 2003) exposed in the northern end of the Serrezuela range (Fig. 1a). In this region, the granite and crystalline basement are locally covered by Upper Paleozoic strata (Tasa Cuna Formation), sedimentary history associated with a Carboniferous uplift, exhumation and the development of a glacial paleovalley (Astini and Del Papa, 2014). The following sedimentary pile is represented by thin (<500 m thick) alluvial Cretaceous and Cenozoic successions that rest on the crystalline basement, overstepping the Serrezuela/Tasa Cuna area. The uppermost Cretaceous to Neogene sedimentary strata were associated with the latest tectonic events reported in the eastern Sierras Pampeanas: rift basins formed during the opening of the Atlantic Ocean, which were tectonically inverted during Andean compression (see Schmidt et al., 1995, Martino et al., 2016; Canelo et al., 2019). Along and across the eastern Sierras Pampeanas, no Triassic and Jurassic records crop out, suggesting that an extended erosional/no depositional event would have dominated these latitudes between the Late Paleozoic and Cretaceous, during the amalgamation-breakup of Pangea. Two other areas (Fig. 1a) were analyzed further south along the same thrust sheet, in the Pocho and Yacanto areas (see Löbens et al., 2011a,b, 2017; Bense et al., 2013). In these regions, as in other parts of the eastern Sierras Pampeanas, there are not (or a few) Late Paleozoic strata covering the Proterozoic-Paleozoic basement intruded by Middle-Late Paleozoic granites (Baldo and Verdecchia, 2014; Gomez, 2003; Dahlquist et al., 2018). Only very local and thin patches of Cretaceous or Cenozoic rest on the crystalline substrate.

Although no major sedimentary records were reported during the Triassic and Jurassic, published low-temperature thermochronology from easternmost Sierras Pampeanas (Löbens et al., 2011a,b, 2017; Bense et al., 2013; Dávila et al., submitted) and thermobarometric modeling of poorly fractionated basalts localized in Triassic rift basins might assist us in interpreting the geodynamic scenario that gave place to this major geological discontinuity.

3. Methodology

Our studies are based on two main approaches: (1) A multisample thermochronological modelling (see Tables SM1 and SM2) using the software QTQt (Gallagher, 2012) and (2) thermobarometric modelling of melting conditions in the mantle (Table SM3).

3.1. AFT age modelling

Previous modeling attempts in the westernmost Sierras de Córdoba thrust sheet have used multi-method (i.e., (U–Th)/He and fission-track) data from individual samples with no geologic constraints (Bense et al., 2013; Löbens et al., 2011a,b) to reproduce possible thermal paths. In contrast, we conducted multi-sample modeling of published data along three localities (Löbens et al., 2011a,b and Bense et al., 2013; Dávila et al., submitted), including vertical profiles, and considered different initial conditions. These constraints included (1) the age and emplacement temperature of the Early Carboniferous granites (356 ± 3 Ma, Dahlquist et al., 2018), and, optionally, (2) residence at near-surface temperatures in Upper Carboniferous times, as documented by the presence of Pennsylvanian strata unconformably overlying the analyzed samples. The southernmost samples (Yacanto and Pocho areas; Fig. 1a) are from the metamorphic basement and consist of two age-elevation profiles totaling 6 AFT samples, and (U–Th)/He ages in 7 zircon samples (ZHe, 22 aliquots) and 10 apatite samples (AHe, 29 aliquots). In contrast, the sample coming from the north (Dávila et al., submitted), in

the Serrezuela range, is a single specimen collected from a lower Carboniferous granite and comprises AFT data only. We conducted inverse modeling of low-temperature thermochronnological data using the QTQt software (Gallagher, 2012). As the central and southern profiles did not include all raw data needed for modeling, (single-grain AFT ages, track length measurements, kinetic parameters, and the dimensions (U–Th)/He aliquots dimensions), we resampled single grain AFT ages based on reported central ages, total number of spontaneous and induced tracks (Ns, Ni), the number of grains dated and other parameters (Rho-D, ND, and zeta). Likewise, we resampled individual track lengths based on published histograms, the mean track length (MTL) values and the number of confined tracks measured. In addition, as crystal dimensions for each (U–Th)/He aliquot were not available in the published works, we calculated the dimensions for hexagonal prisms of equal length and width, based on the alpha-ejection correction factor (Ft) provided by Löbens et al. (2013), and by matching the aliquot volume that we calculated from the data in Bensen et al. (2013) using mineral densities of 3.15 g/cm^3 and 4.65 g/cm^3 for apatite and zircon, respectively.

To facilitate the comparison of results, initial and final temperatures for the thermal histories were defined for all localities. In the north and central profiles, residence at a temperature higher than the closure temperature of the ZHe system (280 ± 40 °C) at the time granite intrusion (350 ± 10 Ma, according to U–Pb data, Dahlquist et al., 2018, see also Geological setting) and a present-day temperature of 10 ± 5 °C were considered. For the southern profile, which comprises samples in granitoids and their lower Paleozoic metamorphic host rocks, residence at 290 ± 10 °C during metamorphic ages of 460 ± 10 Ma (Sims et al., 1998) was used. Two intermediate constraints ("model boxes") were set within the modeling window to simulate sedimentation of Pennsylvanian postglacial units between 320 ± 10 Ma (cf. Astini and Del Papa, 2014). However, we performed sensibility tests by running simulations without any other geological constraint apart from the higher temperature constraint for each model (dashed t-T paths in Fig. 2). We used the multi-compositional fission-track annealing model of Ketcham et al. (2007), and the radiation damage models of Flowers et al. (2009) and Guenthner et al. (2013) for Helium diffusion in apatite and zircon, respectively.

3.2. Thermobarometric modelling

Many thermobarometric methods have been developed to determine the pressure (P) and temperature (T) conditions for basaltic magma generation in equilibrium with a peridotite source (e.g., Lee et al., 2009; Putirka, 2008; Putirka et al., 2018; Plank and Forsyth, 2016; Till et al., 2013). However, the temperature difference among them is ~50 °C and low for our objective of determining whether the mantle potential temperature during the Triassic was anomalously hot or not. We used the Si and Mg thermobarometer of Plank and Forsyth (2016) that, in addition, allowed us calculating the melting depth, which is a key parameter to understand the response of the lower part of the lithosphere to stretching and changes of lithospheric thickness. Geochemical data (Table SM3) are from the southernmost Ischigualasto basin in the Sierra de Valle Fertil (Castro de Machuca et al., 2019, Fig. 1a) and Cuyo basin (Orellano et al., 2019; Ramos and Kay, 1991 and our sample), located close to the Andean belt. Only samples with MgO >7 wt% (or mg# [molar MgO/(MgO + FeO*) x 100] > 55) were used for modeling to avoid major clinopyroxene fractionation and crustal contamination (mg# is the Mg-number and FeO* is the total Fe). However, few differences are observed when considering a cutoff of MgO >6 wt% (see Table SM3). The few reported olivine data (Castro de Machuca et al., 2019), in turn, indicate that the Ni content is low, similar to the most evolved MORBs (cf., Sobolev et al., 2005), suggesting a peridotitic rather than a pyroxenitic mantle source for the selected mafic rocks. We assumed a H2O content of 0.5%, typical of alkaline magmas and consistent with the calculated Ne-normative mineralogy (Castro de Machuca et al., 2019). Before performing the thermobarometric calculations, the basalt compositions were corrected for olivine fractionation by 0.001% incremental addition of olivine until obtaining a Fo_{90} olivine composition using an Fe–Mg olivine-melt partition coefficient of 0.3 and a Fe^{3+}/Fe^* ratio of 0.15. For the lithospheric thickness calculation, we used an average thickness crust of 30 km and densities of 2.85 and 3.25 for the crust and lithospheric mantle, respectively. An isobaric fractional crystallization modeling was also performed in order to test the relationship between basalts from Cuyo and Ischigualasto regions. The result that best fits our samples was obtained using the Amoeba routine in the Alphamelts program (Smith and Asimow, 2005; Antoshechkina et al., 2010) with pressure sets to 10000 bars and an oxygen fugacity at QFM buffer (Fig., S1). Data handling and plots were carried out using the GCDkit program (Janoušek et al., 2006).

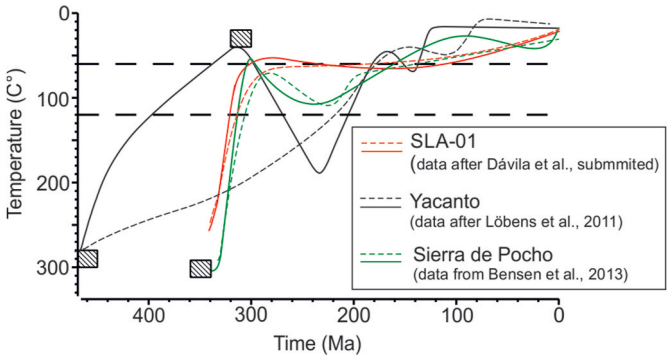

Fig. 2. Thermochronological modelling of (a) Davila et al. (submitted) sample (red line), and data from (b) Bense et al. (2013; green line) and (c) Löbens et al. (2011; black line). Solid lines show results using geological constraints (boxes) whereas dashed lines depict results without stratigraphic constraints. (For interpretation of the references to colour in this figure legend, the reader is referred to the Web version of this article.)

4. Results

4.1. AFT age modelling

The best-fit thermal history using the sample from the northern part of the Pocho-Serrezuela thrust sheet (Dávila et al., submitted) as well as multisample thermal histories extracted from vertical profiles on specimens collected southward along the Sierra de Pocho to Yacanto sections (Bense et al., 2013 and Löbens et al., 2011a,b) show a clear pattern: A rapid Carboniferous cooling (after granite crystallization) followed by moderated Triassic reheating and Jurassic-early Cretaceous cooling (see Fig. 2; Dávila et al., submitted). Our results suggest that after late Paleozoic exhumation the northernmost samples (i.e., Serrezuela and Pocho, see Fig. 1a) were never (totally or partly) reset, however, there was a total resetting of the AFT and ZHe systems for the samples collected to the South (i.e., Yacanto, see Fig. 1a). Moreover, it is important to notice that the reported patterns and central ages were also modelled without constraints showing the similar results (see dashed lines in Fig. 2) for two of the three localities, attesting to the robustness of the thermal path signatures. In the northernmost profile (Yacanto), the unconstrained model does not require Paleozoic cooling and hence it does not require Triassic heating either. Despite the inherent non-uniqueness of thermal histories in thermochonologic modeling (Ketcham et al., 2009), a more reliable model is that which honors both the thermochronological data and the geologic constraints. We thus prefer the constrained model, as it includes residence at near-surface temperatures during the Carboniferous, as supported by stratigraphic evidence (Fig. 1C)

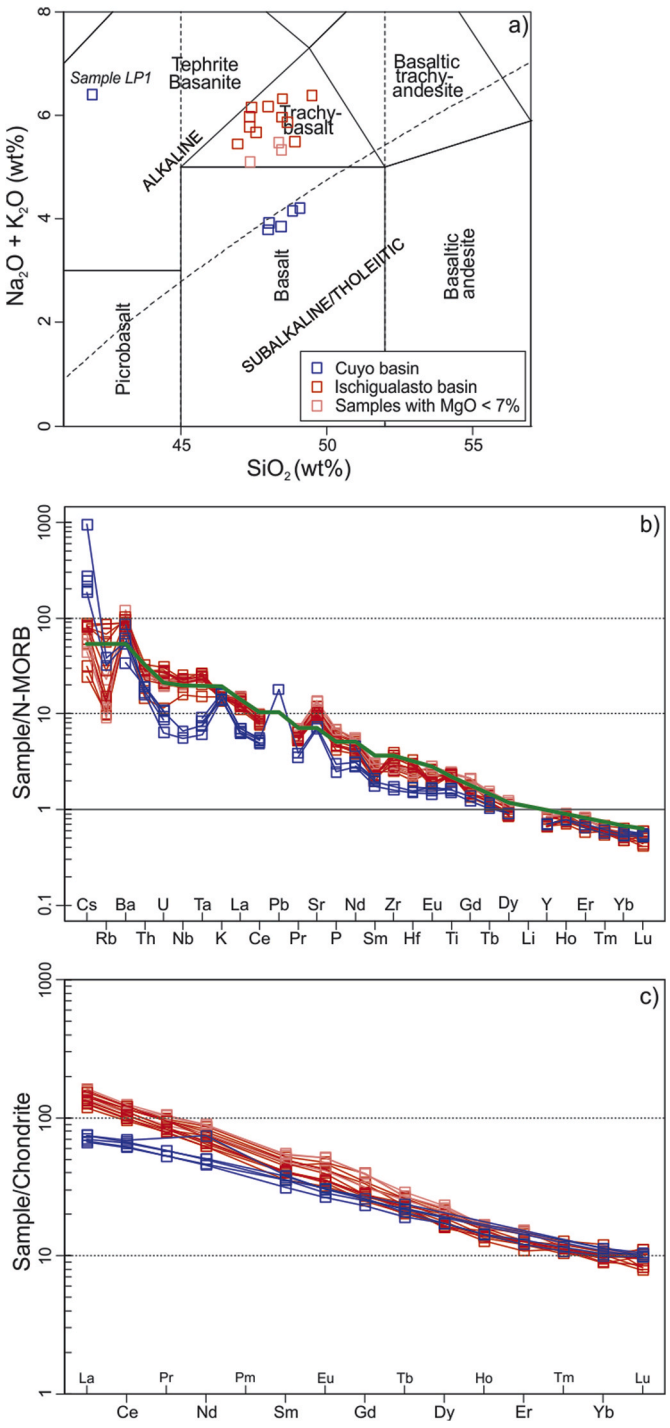

Fig. 3. (a) Total alkali-silica (TAS) diagram with indication of alkaline and subalkaline fields after Irvine and Baragar (1971), (b) NMORB-normalized trace element diagram and (c) chondrite-normalized REE diagram for the Triassic basalts dataset. NMORB and REE normalization factors are from Sun and McDonough (1989) and Anders and Grevesse (1989), respectively. The green solid line in Fig. 3b is the OIB composition (Sun and McDonough, 1989) for comparison. (For interpretation of the references to colour in this figure legend, the reader is referred to the Web version of this article.)

4.2. Basalt geochemistry and thermobarometry

According to geochemical compositions, the Triassic basalts of western Sierras Pampeanas are mantle derived without a strong influence of crustal contamination (Ramos and Kay, 1991; Castro de Machuca et al., 2019). Such types of basalts provide a good record of the pressure and temperature conditions during mantle melting (Herzberg et al., 2007). The Triassic lavas used for modelling are Mg-rich and most plot as slightly alkaline basalts and trachy-basalts in the TAS diagram (Le Bas et al., 1986, Fig. 3a). The relatively high Cr (137–334) and Ni (97–182) contents of the selected samples suggest that they only experienced olivine and minor clinopyroxene fractionation. All lavas show enrichment of incompatible trace elements (Fig. 3b) and low Th/Nb and La/Nb ratios (<0.15), values that are similar to OIB magmas and most within-plate basalts. The high medium to heavy REE ratios, in turn, indicate melting in the garnet stability field of the mantle (>70 Km) although Ischigualasto samples show higher La_N/Yb_N ratios (average = 17.3) than the samples from Cuyo basin (average = 6.1). The isotopic composition points to a HIMU (high μ, $\mu = {}^{238}U/{}^{204}Pb$) mantle reservoir for the Triassic basalts (Castro de Machuca et al., 2019). The lavas from both analyzed regions are well related by fractional crystallization processes according to our major elements modelling using the Alphamelts program run under high pressure conditions (Fig. SM1), as suggested by the REE composition. The calculated P-T conditions (see the methodology section) indicate that lavas from Ischigualasto basin equilibrated in the mantle at 1406 ± 26.9 °C and 2.68 ± 0.13 GPa, while Cuyo basin basalts yielded values of 1390 ± 11.6 °C and 2.26 ± 0.11 GPa. These temperatures are within the normal mantle potential temperature (1320–1420 °C), as recorded in MORB (Cottrell and Kelley 2011). In addition, they are considered as maximum values. Any fractionation of clinopyroxene (not considered in our calculations) would result in an increase in the calculated mantle temperature of up to 100 °C (Herzberg et al., 2007). The high pressure melting conditions determined here, on the other hand, are consistent with the REE geochemistry, but also with our fractional crystallization modeling. However, the calculated pressure values indicate that the stretching was larger in the Cuyo basin. An average lithospheric thickness of ~75 km and ~88 km was obtained for Cuyo and Ischigualasto basins, respectively, using a conservative 30 km crustal thickness. A higher crustal thickness would result in a thicker lithospheric lid. Similar values were obtained for the Cuyo basin based on REE geochemical data (Orellano et al., 2019).

5. Discussion

As it was mentioned in the introduction section, one of the widely identified geological features of central Argentina, particularly in the Sierras Pampeanas, is the lack of Triassic and Jurassic stratigraphic records. This has allowed defining a regional discordance ("the Pampean unconformity", Jordan et al., 1989), which implies a long lapse of erosion or no sedimentation (depositional hiatus). Both situations, however, do not generate the same thermal cooling histories and exhumation paths. While the first scenario (erosion) could provide cooling paths contemporaneous with the eroded levels, the second situation (no sedimentation) could hardly do it.

Fortunately, thermochronology provides cooling ages of rocks and, with appropriate modeling, allows to constrain the moment when a mineral (included in a bedrock) passes through a specific closure temperature (Dodson, 1973). The thermochronometres used in this contributions (ZHe, AFT and AHe) allow characterizing the thermal history of the shallowest crust (given that the closure temperatures are between 60° and 200 °C, i.e., ~2–7 km from the surface, assuming average geothermal gradients). It is important to take into account that Exhumation (E), surface (SU) and rock (RU) uplift are closely related: SU = RU - E (England and Molnar, 1990). Exhumation, in turn, relates directly to denudation and erosion, which require a relief to be created. Surface uplift, then, results from the interaction of RU and E. A cooling path derived from thermochronological modeling, therefore, might evidence erosional stages but indirectly tectonic processes (uplift) generated before or during erosion. Cooling can be also related to changes of the thermal conditions of the lithosphere (crust and/or mantle). A basal heat flow change might impact in the thermal state and, consequently, in the

cooling ages (see Dávila and Carter, 2013, Sanchez Nassif et al., this volume). This means that a thermochronological heating/reheating event could be connected with burial or heat flow increase, or a combination of both.

Our results show a clear Triassic reheating episode followed by a Jurassic to Cenozoic slow cooling. Our models (see Fig. 2) also document that the associated peak temperatures during this Triassic event were cooler (~60 °C) in the north (Serrezuela; Fig. 1a) than toward the south (Pocho and Yacanto areas, ~100° and ~200 °C, respectively). Considering that the sampling areas are part of the same basement thrust sheet, ~200 km apart from each other, the contrasting temperatures along strike might be associated with the depth of the samples during the Triassic resetting. Similar AFT ages (237 and 208 Ma) have been described further north in the Sierras Pampeanas, in the Ancasti range (see Jordan et al., 1989) as well as in other areas of the Sierras Pampeanas (see Fig. 4 of Dávila and Carter, 2013). But the thermal modelling shows the beginning of the discordance formation was relatively coeval with a Triassic reheating. Although the Jurassic cooling history is consistent with the discordance evolution, a Triassic reheating without strata requires a mechanism different from burial heating. This interpretation would require a large amount of subsidence and sedimentary successions, not reported at the moment in the Sierras de Córdoba and nearby areas. To achieve the variable degrees of resetting (supported by the modeling results) after the Late Paleozoic basin stage (using an average geotherms of ~25 °C/km) a southward thickening sedimentary pile of 2–7 km would be needed (AFT closure temperature is 120–90 °C). As mentioned above, only localized Triassic extensional basins have been reported westward from the Sierras Pampeanas, closer to the Andean belt.

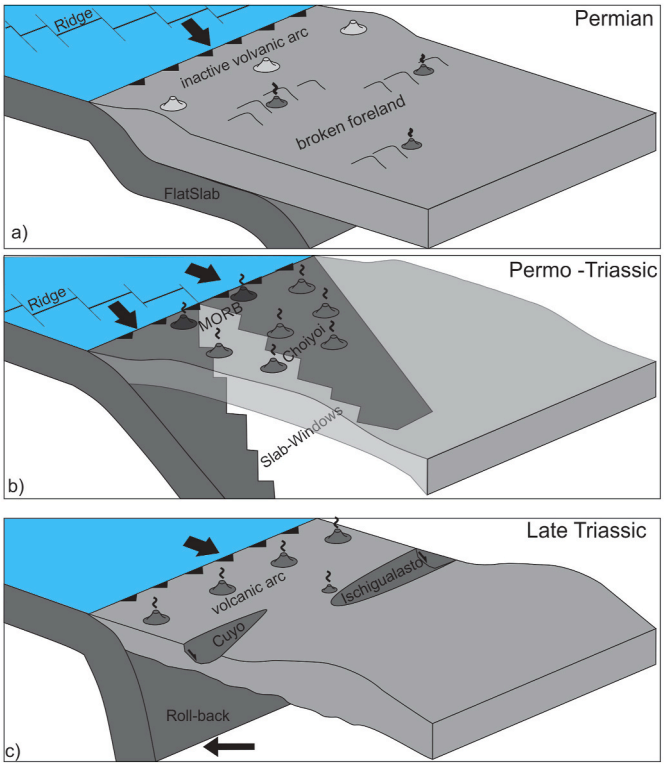

Fig. 4. Geodynamic evolution of Western Gondwana from the Late Permian to Late Triassic (likely Jurassic). Our model proposes (a) Permian flat subduction (cf. del Rey et al., 2016) followed by (b) the subduction of a seismic ridge and formation of a slab window in the Permo-Triassic (MORB-type magmas in the fore-arc region) and later (c) rollback during the Late Triassic. While an slab window scenario allows explaining the moderate Triassic reheating, uplift and formation of a major discordance across the foreland, the subsequent slab rollback can be related with backarc extension and formation of extensional basins (Ischigualasto and Cuyo basins). The black arrows in the oceanic zone indicate the plate motion.

Recently, high heat flow conditions (~90 mW/m2) were determined using clays and vitrinite modelling (Ezpeleta et al., 2019) at shallow crustal levels within the Triassic Ischigualasto basin (at the Triassic bottom). Such an increase in paleo-heat flow could explain the reset (at least partly) of the late Paleozoic thermochronologic ages (see Bense et al., 2013; Dávila et al., submitted). However, there are a large number of geodynamic processes that could explain an increase in heat flow, as increases of radiogenic heat production or geothermal gradient.

High heat flow conditions, in the study area, cannot be the result of radiogenic heat production of crustal materials. The last major felsic event occurred in the Mississippian (Dahlquist et al., 2013), ~100 million of years before the Triassic reheating reported in this contribution. Two major aspects, however, do not agree with this hypothesis: (i) The radiogenic total flux decays in 10–20 my (Artemieva and Mooney, 2001) and (ii) this process can not necessarily be associated with rifting or regional uplift.

A mantle plume scenario could also generate a geothermal gradient increase. However, this scenario is ruled out as our thermobarometric calculations on basalts exposed in Ischigualasto and Cuyo basins show "normal" Triassic mantle potential temperatures and suggest that volcanism would be a passive response to extension. We interpret this homogeneous thermal state as the result of a rapid extraction from a geochemically isolated mantle reservoir, in accordance with the local extensional tectonics.

Therefore, the only suitable explanation for the Triassic reheating is to shorten the distance between the mantle and surface isotherms, which would lead to an increase of the geotherm and surface heat flow. The model that best fits our data is a degradation of the lithosphere base (Putirka et al., 2012), either by rollback and subsequent delamination or by slab windows. Both processes might explain the heating paths derived from thermochronology modelling, surface uplift and the ensuing regional unconformity development during the Triassic of west-central Argentina. Trace element ratios and available isotopic data of the studied Triassic basalts (Ramos and Kay, 1991; Alexandre et al., 2009; Castro de Machuca et al., 2019, Orellano et al., 2019) and coeval intrusive rocks from central Chile (del Rey et al., 2016) support an asthenospheric mantle upwelling since the latest Permian and complete removal of the lithosphere at ~230 Ma (see Fig. 3 in del Rey et al., 2016). However, both models have some weak points. The evolution from shallow to steep subduction (or rollback, e.g., Royden, 1993) could reproduce the extensional tectonics close to the continental margin (Nakakuki and Mura, 2013; Schellart and Moresi, 2013; Cassel et al., 2018), as previously suggested by other authors in western Argentina (Castro de Machuca et al., 2019; Orellano et al., 2019). In fact, the Cuyo basin basalts, located further west of the Ischigualasto basin, display a slight negative Nb–Ta anomaly (Fig. 3b) and higher Th/Nb ratios, indicative of the presence of a deep subduction component (Pearce and Stern, 2006). According to recent models, back arc basins occur when the retreating slab stagnates at the mantle transition zone (Nakakuki and Mura, 2013), a region from where the HIMU-type magmas, similar to the studied basalts, are strikingly sourced (Huang et al., 2020). Although changes of subduction angles have been recurrently described in the evolution of the Andean margin (Ramos and Folguera, 2009), a delamination process to explain the uplift requires, in addition, a previous shortening and lithosphere thickening (e.g., in the Permian-Lower Triassic) to eclogitize the lower crust (Kay and Kay, 1993; Krystopowicz and Currie, 2013). Proximal volcaniclastic records exposed in Permian red beds of the eastern Sierras Pampeanas, suggested a volcanism far from the Late Paleozoic continental margin and an Early-Middle Permian flat subduction (Astini et al., 2005). The same scenario was recently proposed south of 31° SL based on an eastward migration of the magmatism in Chile (del Rey et al., 2016). This slab flattening is also an alternative model to account for the Permo-Triassic San Rafael deformation (Llambí as and Sato, 1995), particularly in foreland regions

located far away from the main orogenic belt (Dávila et al., 2003; Astini et al., 2005). However, this event has not been recorded in the Sierras Pampeanas region. According to this proposal, a subsequent slab retreat and rollback would have triggered the extensive flare-up and deposition of the late Permian-Early Triassic Choiyoi volcanics and granites (Kay and Mpodozis, 2002). Later mantle delamination is likely the easiest explanation to generate uplift and account for the Triassic unconformity formation, a hypothesis that needs to be tested.

Conversely, the development of a slab window during the Triassic in response to the subduction of a seismic ridge (see Müller et al., 2016) might account for a lithospheric thickness reduction, isostatic rebound (uplift) and increase of surface heat flow (Ávila and Dávila, 2018, 2020) without requiring slab flattening and delamination stages. The southward increase in paleotemperatures (~60 °C to the north and ~200 °C to the south) recorded by our thermochronologic modelling (Fig. 2) might be associated with either the geometry or kinematics of this asthenospheric window (e.g., Goddard and Fosdick, 2019) but also with faulting and surface tectonics. The slab windows hypothesis is supported by the presence of Triassic MORB-type toleites interbedded with marine strata in the Cordillera de la Costa of central Chile (Vergara et al., 1991; Morata et al., 2000). These are typical compositions in modern margins affected by the subduction of ridges (Thorkelson and Breitsprecher, 2005). Furthermore, Triassic shoshonites from NW La Pampa province (Llambıas et al., 2003), >400 km from the coeval continental margin, show adakite-like geochemical features such as $SiO2 \geq 56\%$, $Al2O3 \geq 15\%$, $Na2O \geq 3\%$, $Sr \geq 400$ ppm, $Y \leq 18$ ppm, $Yb \leq 1.8$ ppm (Castillo, 2012). The presence of adakites is also consistent with our model, although we cannot rule out an origin linked with the Permian flat slab stage. Unfortunately, the geochemical data (La_N/Yb_N vs Sr/Y ratios) is not conclusive as to whether they resulted from the melting of an oceanic slab or a lower crust. On the other hand, the slab windows alternative hardly explains the development of extensional basins along the continental margin. Although local stretching might occur associated with the plate kinematics across of the main ridge and related transform faults (see Georgieva et al., 2019), the few sub-recent analogues (in Patagonia, for example) do not show major rift basins. Considering that the available data is not conclusive to support one of the proposed alternatives, we cannot disregard a combination of a seismic ridge subduction and slab rollback to account for the different observations stated above, as suggested for the Cretaceous magmatism of eastern China (Ling et al., 2013), also located far from the contemporaneous subduction zone. It is well known that flat slabs can be produced by subduction of buoyant, young and hot oceanic plates adjacent to spreading ridges (Gutscher et al., 2000; Espurt et al., 2008; Manea et al., 2017; among others). This supports our hypothesis and model (Fig. 4).

The slab window and rollback hypotheses, in addition to account for an increase of temperature, agree with a reduction of temperature and heat flow in the upper crust during the evolution. After crustal reheating and uplift, erosion might conduct exhumation of the sampled levels, which allows explaining the subsequent Jurassic cooling event. Finally, our interpretation is also consistent with a recent work further south (Gianni et al., 2019), which proposes a slab tear to explain the opening of the Neuquén and Colorado basins during the Upper Triassic based on geochemical and geophysical data.

6. Conclusions

Our work analyzes one of the major unconformities from central Argentina, developed between the Upper Permian and Cretaceous. In outcrops, it is represented by Cretaceous clastics overlying lower Permian red beds. This episode has been poorly (or not) analyzed in geological studies of the Sierras Pampeanas, given the lack of clear geological evidence. On the base of our thermochronological modelling, we defined a reheating event in the Triassic, without evidence of burial, followed by a Jurassic-Cretaceous cooling. We also show, from petrogenetic studies on Triassic basalts that the asthenospheric mantle had average potential temperatures similar to MORBs. Considering extensional basins near the continental margin and that high heat flows have been reported during this episode, we proposed a geodynamic model dominated by slab window and/or rollback followed by delamination, which produced a reduction of the lithospheric weight and isostatic rebound. This uplift and erosion drove the exhumation during the remaining Triassic and Jurassic.

Author statement

F. Martina and F. Dávila conceived the idea. FM performed the petrogenetic modeling and wrote the first draft of the paper. P Ávila and FD performed the thermochronological modeling and M. Parra obtained the AFT data. PA was also in charge of the figures, references and data presentation. All authors contributed equally to the discussion of the results and to the conclusions of this study. I confirm that the manuscript has been read and approved by all named authors. I confirm that the order of authors listed in the manuscript has been approved by all named authors. The Corresponding Author declared on the title page of the manuscript is: Dr. Federico Martina.

Declaration of competing interest

The authors declare that they have no known competing financial interests or personal relationships that could have appeared to influence the work reported in this paper.

Acknowledgements

We thank CONICET grant PUE-2016 (to CICTERRA), FONCYT grant PICT-2015-1092 and UNC for supporting this research. Themochronometric analyses were funded by the FAPESP-CONICET SPRINT Project 2016/50441-1. Leandro Gilli assisted with the field work in the Cuyo basin and during sample preparation. Editor and reviewer comments improve our manuscript.

Appendix A. Supplementary data

Supplementary data to this article can be found online at https://doi.org/10.1016/j.jsames.2020.102956.

References

Alexandre, F.P., Sommer, C.A., Lima, E.F., Chemale Jr., F., Marsicano, C.A., Mancuso, A. C., Brod, J.A., 2009. Petrologia do magmatismo básico do Cerro Morado na bacia triássica Ischigualasto-Villa Unión (NW da Argentina). Pesqui. em Geociencias 36, 295–313.

Anders, E., Grevesse, N., 1989. Abundances of the elements: meteoritic and solar. Geochem. Cosmochim. Acta 53, 197–214. https://doi.org/10.1016/0016-7037(89)90286-X.

Antoshechkina, P., Asimow, P., Hauri, E., Luffi, P., 2010. Effect of water on mantle melting and magma differentiation, as modeled using Adiabat_1ph 3.0, AGU Fall Meeting Abstracts, p. 2264.

Artemieva, I.M., Mooney, W.D., 2001. Thermal thickness and evolution of Precambrian lithosphere: a global study. J. Geophys. Res.: Solid Earth 106 (B8), 16387–16414.

Astini, R.A., Dávila, F.M., López Gamundí, O., Gómez, F.J., Collo, G., Ezpeleta, M., Martina, F., Ortiz, A., 2005. Frontera Exploratoria de la Argentina. Cuencas de la región precordillerana. Spalletti, Chebli, GA; Cortiñas, JS, pp. 115–146.

Astini, R.A., Del Papa, C.E., 2014. Cubierta sedimentaria paleozoica superior. In: Martino, R.D., Guereschi, A. (Eds.), Relatorio del XIX Congreso Geológico Argentino: Geología y Recursos Naturales de la Provincia de Córdoba. Asociación Geológica Argentina, Córdoba, pp. 393–420.

Avila, J.N., Chemale Jr., F., Mallmann, G., Kawashita, K., Armstrong, R.A., 2006. Combined stratigraphic and isotopic studies of triassic strata, Cuyo basin, Argentine Precordillera. GSA Bull. 118, 1088–1098. https://doi.org/10.1130/B25893.1.

Ávila, P., Dávila, F.M., 2018. Heat flow and lithospheric thickness analysis in the Patagonian asthenospheric windows, southern South America. Tectonophysics 747–748, 99–107. https://doi.org/10.1016/J.TECTO.2018.10.006.

Ávila, P., Dávila, F.M., 2020. Lithospheric thinning and dynamic uplift effects during slab window formation, southern Patagonia (45°-55° S). J. Geodyn. 133, 101689. https://doi.org/10.1016/J.JOG.2019.101689.

Le Bas, M.L., Maitre, R.L., Streckeisen, A., Zanettin, B., 1986. IUGS Subcommission on the Systematics of Igneous Rocks. A chemical classification of volcanic rocks based on the total alkali-silica diagram. J. Petrol. 27 (3), 745–750.
Baldo, E.G., Verdecchia, S.O., 2014. Las metamorfitas de contacto asociadas al magmatismo Aachaliano de las Sierras de Córdoba. In: Martino, R.D., Guereschi, A. (Eds.), Relatorio del XIX Congreso Geológico Argentino: Geología y Recursos Naturales de la Provincia de Córdoba. Asociación Geológica Argentina, Córdoba, pp. 349–363.
Bense, F.A., Löbens, S., Dunkl, I., Wemmer, K., Siegesmund, S., 2013. Is the exhumation of the Sierras Pampeanas only related to Neogene flat-slab subduction? Implications from a multi-thermochronological approach. J. S. Am. Earth Sci. 48, 123–144. https://doi.org/10.1016/j.jsames.2013.09.002.
Canelo, H.N., Nóbile, J.C., Dávila, F.M., 2019. Uplift analysis on a pericratonic region: an example in the Sierras de Córdoba (29°–34°S), Argentina. Geomorphology 329, 81–98. https://doi.org/10.1016/j.geomorph.2018.12.024.
Castillo, P.R., 2012. Adakite petrogenesis. Lithos 134–135, 304–316. https://doi.org/10.1016/j.lithos.2011.09.013.
Castro de Machuca, B., López, M.G., Morata, D., Fuentes, M.G., 2019. Geochemical constraints on the petrogenesis of Triassic alkaline basalts of Sierra de Valle Fértil, Western Sierras Pampeanas, Argentina: implications for their origin, evolution and tectonic setting. J. South Am. Earth Sci vol. 95, 102297. https://doi.org/10.1016/j.jsames.2019.102297.
Cassel, E.J., Smith, M.E., Jicha, B.R., 2018. The impact of slab rollback on Earth's surface: Uplift and extension in the Hinterland of the North American Cordillera. Geophys. Res. Lett. 45, 10,996–11,004. https://doi.org/10.1029/2018GL079887.
Cottrell, E., Kelley, K.A., 2011. The oxidation state of Fe in MORB glasses and the oxygen fugacity of the upper mantle. Earth Planet Sci. Lett. 305, 270–282. https://doi.org/10.1016/j.epsl.2011.03.014.
Dahlquist, J.A., Pankhurst, R.J., Gaschnig, R.M., Rapela, C.W., Casquet, C., Alasino, P.H., Baldo, E.G., 2013. Hf and Nd isotopes in Early Ordovician to Early Carboniferous granites as monitors of crustal growth in the Proto-Andean margin of Gondwana. Gondwana Res. 23 (4), 1617–1630.
Dahlquist, J.A., Alasino, P.H., Basei, M.A.S., Morales Cámera, M.M., Macchioli Grande, M.S., da Costa Campos Neto, M., García Larrecharte, M., 2018. Recurrent intrusive episodes in the Paleozoic metasedimentary upper crust during the Early Carboniferous time: the Veladero granitoid stock and the peraluminous andesite. J. S. Am. Earth Sci. 88, 80–93. https://doi.org/10.1016/j.jsames.2018.08.011.
Dávila, F.M., Carter, A., 2013. Exhumation history of the andean broken foreland revisited. Geology 41, 443–446. https://doi.org/10.1130/G33960.1.
Dávila, F.M., Astini, R.A., Schmidt, C.J., 2003. Unraveling 470 my of shortening in the Central Andes and documentation of Type 0 superposed folding. Geology 31 (3), 275–278.
del Rey, A., Deckart, K., Arriagada, C., Martínez, F., 2016. Resolving the paradigm of the late Paleozoic–Triassic Chilean magmatism: isotopic approach. Gondwana Res. 37, 172–181. https://doi.org/10.1016/j.gr.2016.06.008.
Dodson, M.H., 1973. Closure temperature in cooling geochronological and petrological systems. Contrib. to Mineral. Petrol. Times 40, 259–274.
England, P., Molnar, P., 1990. Surface uplift, uplift of rocks, and exhumation of rocks: Geology 18, 1173–1177.
Espurt, N., Funiciello, F., Martinod, J., Guillaume, B., Regard, V., Faccenna, C., Brusset, S., 2008. Flat subduction dynamics and deformation of the South American plate: insights from analog modeling. Tectonics, 27(3).
Ezpeleta, M., Collo, G., Sanchez Nassif, F., Wunderlin, C., Parra, M., 2019. Thermal Modeling of the Ischigualasto Basin (Triassic of La Rioja, Argentina): Burial, Structuring and Magmatism Controlling the Timing of Petroleum Generation. AAPG ICE Abstracts, Buenos Aires.
Flowers, R.M., Ketcham, R.A., Shuster, D.L., Farley, K.A., 2009. Apatite (U–Th)/He thermochronometry using a radiation damage accumulation and annealing model. Geochem. Cosmochim. Acta 73, 2347–2365. https://doi.org/10.1016/j.gca.2009.01.015.
Gallagher, K., 2012. Transdimensional inverse thermal history modeling for quantitative thermochronology. Journal of Geophysical Research: solid Earth, 117. https://doi.org/10.1029/2011JB008825.
Georgieva, V., Gallagher, K., Sobczyk, A., Sobel, E.R., Schildgen, T.F., Ehlers, T.A., Strecker, M.R., 2019. Effects of slab-window, alkaline volcanism, and glaciation on thermochronometer cooling histories, Patagonian Andes. Earth Planet Sci. Lett. 511, 164–176.
Gianni, G.M., Navarrete, C., Spagnotto, S., 2019. Surface and mantle records reveal an ancient slab tear beneath. Gondwana. Sci. Rep 9, 1–10. https://doi.org/10.1038/s41598-019-56335-9.
Goddard, A.L., Fosdick, J.C., 2019. Multichronometer thermochronologic modeling of migrating spreading ridge subduction in southern Patagonia. Geology 47, 555–558. https://doi.org/10.1130/G46091.1.
Gómez, G.M., 2003. El plutón de Serrezuela: evento magmático del Carbonífero en el sector norte de la Sierra de Pocho, Córdoba, República Argentina. Revista de la Asoc Geol Argent 58 (3), 283–297.
Gordillo, C.E., Lencinas, A.N., 1979. Sierras Pampeanas de Córdoba y san luis. Geología Regional Argentina 1, 577–650.
Guenthner, W.R., Reiners, P.W., Ketcham, R.A., Nasdala, L., Giester, G., 2013. Helium diffusion in natural zircon: radiation damage, anisotropy, and the interpretation of zircon (U-Th)/He thermochronology. Am. J. Sci. 313, 145–198.
Gutscher, M.A., Maury, R., Eissen, J.P., Bourdon, E., 2000. Can slab melting be caused by flat subduction? Geology 28 (6), 535–538.
Herzberg, C., Asimow, P.D., Arndt, N., Niu, Y., Lesher, C.M., Fitton, J.G., Saunders, A.D., 2007. Temperatures in ambient mantle and plumes: Constraints from basalts, picrites, and komatiites. Geochem. Geophys. Geosyst. 8 https://doi.org/10.1029/2006GC001390.
Huang, S., Tschauner, O., Yang, S., Humayun, M., Liu, W., Gilbert Corder, S.N., Bechtel, H.A., Tischler, J., 2020. HIMU geochemical signature originating from the transition zone. Earth Planet Sci. Lett. 542 (116323) https://doi.org/10.1016/j.epsl.2020.116323.
Hyppolito, T., Juliani, C., Garcia-Casco, A., Meira, V., Bustamante, A., Hall, C., 2015. LP/HT metamorphism as a temporal marker of change of deformation style within the Late Palaeozoic accretionary wedge of central Chile. J. Metamorph. Geol. 33 (9), 1003–1024.
Irvine, T.N.J., Baragar, W.R.A., 1971. A guide to the chemical classification of the common volcanic rocks. Can. J. Earth Sci. 8 (5), 523–548.
Janoušek, V., Farrow, C.M., Erban, V., 2006. Interpretation of whole-rock geochemical data in igneous geochemistry: introducing geochemical data toolkit (GCDkit). J. Petrol. 47, 1255–1259. https://doi.org/10.1093/petrology/egl013.
Jordan, T.A., Zeitler, P., Ramos, V.A., Gleadow, A.J.W., 1989. Thermochronometric data on the development of the basement peneplain in the Sierras Pampeanas. Argentina. J. South Am. Earth Sci 2, 207–222. https://doi.org/10.1016/0895-9811(89)90030-8.
Kay, R.W., Kay, S.M., 1993. Delamination and delamination magmatism. Tectonophysics 219 (1–3), 177–189.
Kay, S.M., Mpodozis, C., 2002. Magmatism as a probe to the Neogene shallowing of the Nazca plate beneath the modern Chilean flat-slab. J. S. Am. Earth Sci. 15 (1), 39–57.
Ketcham, R.A., Carter, A., Donelick, R.A., Barbarand, J., Hurford, A.J., 2007. Improved modeling of fission-track annealing in apatite. Am. Mineral. 92 (5–6), 799–810.
Ketcham, R.A., Donelick, R.A., Balestrieri, M.L., Zattin, M., 2009. Reproducibility of apatite fission-track length data and thermal history reconstruction. Earth Planet Sci. Lett. 284 (3–4), 504–515.
Krystopowicz, N.J., Currie, C.A., 2013. Crustal eclogitization and lithosphere delamination in orogens. Earth Planet Sci. Lett. 361, 195–207.
Lee, C.T.A., Luffi, P., Plank, T., Dalton, H., Leeman, W.P., 2009. Constraints on the depths and temperatures of basaltic magma generation on Earth and other terrestrial planets using new thermobarometers for mafic magmas. Earth Planet Sci. Lett. 279 (1–2), 20–33.
Ling, M.-X., Li, Y., Ding, X., Teng, F.-Z., Yang, X.-Y., Fan, W.-M., Xu, Y.-G., Sun, W., 2013. Destruction of the North China craton induced by ridge subductions. J. Geol. 121, 197–213. https://doi.org/10.1086/669248.
Llambías, E.J., Sato, A.M., 1995. El batolito de Colangüil: transición entre orogénesis y anorogénesis. Rev. Asoc. Geol. Argent. 50 (1–4), 111–131.
Llambıas, E.J., Quenardelle, S., Montenegro, T., 2003. The Choiyoi Group from central Argentina: a subalkaline transitional to alkaline association in the craton adjacent to the active margin of the Gondwana continent. J. S. Am. Earth Sci. 16 (4), 243–257.
Löbens, S., Bense, F.A., Wemmer, K., Dunkl, I., Costa, C.H., Layer, P., Siegesmund, S., 2011a. Exhumation and uplift of the Sierras Pampeanas: preliminary implications from K–Ar fault gouge dating and low-T thermochronology in the Sierra de Comechingones (Argentina). Int. J. Earth Sci. 100 (2–3), 671–694.
Löbens, S., Bense, F.A., Wemmer, K., Dunkl, I.I., Costa, C.H., Layer, P., Siegesmund, S., 2011b. Exhumation and uplift of the Sierras Pampeanas: preliminary implications from K-Ar fault gouge dating and low-T thermochronology in the Sierra de Comechingones (Argentina). Int. J. Earth Sci. 100, 671–694. https://doi.org/10.1007/s00531-010-0608-0.
Löbens, S., Bense, F.A., Dunkl, I.I., Wemmer, K., Kley, J., Siegesmund, S., 2013. Thermochronological constraints of the exhumation and uplift of the Sierra de Pie de Palo, NW Argentina. J. South Am. Earth Sci. 48, 209–219. https://doi.org/10.1016/j.jsames.2013.09.005.
Löbens, S., Oriolo, S., Benowitz, J., Wemmer, K., Layer, P., Siegesmund, S., 2017. Late Paleozoic deformation and exhumation in the Sierras Pampeanas (Argentina): 40 Ar/39 Ar-feldspar dating constraints. Int. J. Earth Sci. 106 (6), 1991–2003.
Manea, V.C., Manea, M., Ferrari, L., Orozco-Esquivel, T., Valenzuela, R.W., Husker, A., Kostoglodov, V., 2017. A review of the geodynamic evolution of flat slab subduction in Mexico, Peru, and Chile. Tectonophysics 695, 27–52.
Martínez, R.N., Colombi, C.E., 2011. Evolución litofacial y edad de la Formación Cañón del Colorado (Jurásico Inferior), Precordillera oriental, San Juan. Rev. Asoc. Geol. Argent. 68 (1), 95–107.
Martino, R.D., Guereschi, A.B., Montero, A.C., 2016. Reactivation, inversion and basement faulting and thrusting in the Sierras Pampeanas of Córdoba (Argentina) during Andean flat-slab deformation. Geol. Mag. 153 (5–6), 962–991.
Morata, D., Aguirre, L., Oyarzun, M., Vergara, M., 2000. Crustal contribution in the genesis of the bimodal Triassic volcanism from the Coastal Range, central Chile. Rev. Geol. Chile 27 (1), 83–98.
Mpodozis, C., Ramos, V.A., 2008. Tectónica jurásica en Argentina y Chile: extensión, subducción oblicua, rifting, deriva y colisiones? Rev. Asoc. Geol. Argent. 63 (4), 481–497.
Müller, R.D., Seton, M., Zahirovic, S., Williams, S.E., Matthews, K.J., Wright, N.M., Bower, D.J., 2016. Ocean basin evolution and global-scale plate reorganization events since Pangea breakup. Annu. Rev. Earth Planet Sci. 44, 107–138.
Nakakuki, T., Mura, E., 2013. Dynamics of slab rollback and induced back-arc basin formation. Earth Planet Sci. Lett. 361, 287–297.
Orellano, R.A.P., Rubinstein, N.A., Carrasquero, S.I., 2019. Petrogenesis of the Triassic Cuyo basin magmatism: controls on the magmatic evolution of passive rifts basins in Western Gondwana. J. South Am. Earth Sci, 92, 586–597. https://doi.org/10.1016/j.jsames.2019.03.017.
Pearce, J.A., Stern, R.J., 2006. Origin of back-arc basin magmas: trace element and isotope perspectives. Geophys. Monogr. 166, 63–86.

Plank, T., Forsyth, D.W., 2016. Thermal structure and melting conditions in the mantle beneath the Basin and Range province from seismology and petrology. Geochemistry, Geophys. Geosystems 17, 1312–1338.

Putirka, K.D., 2008. Thermometers and barometers for volcanic systems. Rev. Mineral. Geochem. 69 (1), 61–120.

Putirka, K., Jean, M., Cousens, B., Sharma, R., Torrez, G., Carlson, C., 2012. Cenozoic volcanism in the Sierra Nevada and Walker Lane, California, and a new model for lithosphere degradation. Geosphere 8 (2), 265–291.

Putirka, K., Tao, Y., Hari, K.R., Perfit, M.R., Jackson, M.G., Arevalo Jr., R., 2018. The mantle source of thermal plumes: trace and minor elements in olivine and major oxides of primitive liquids (and why the olivine compositions don't matter). Am. Mineral. 103 (8), 1253–1270. https://doi.org/10.2138/am-2018-6192.

Ramos, V.A., 2009. Anatomy and global context of the Andes: main geologic features and the Andean orogenic cycle. Mem. Geol. Soc. Am. 204, 31–65.

Ramos, V.A., Folguera, A., 2009. Andean flat-slab subduction through time. Geol. Soc. Spec. Publ. 327, 31–54.

Ramos, V.A., Kay, S.M., 1991. Triassic rifting and associated basalts in the Cuyo basin, central Argentina. Spec. Pap. Geol. Soc. Am. 265, 79–91.

Richardson, T., Ridgway, K.D., Gilbert, H., Martino, R., Enkelmann, E., Anderson, M., Alvarado, P., 2013. Neogene and quaternary tectonics of the eastern Sierras Pampeanas. Tectonics, vol. 32. Active intraplate deformation inboard of flat-slab subduction, Argentina, pp. 780–796. https://doi.org/10.1002/tect.20054.

Royden, L.H., 1993. Evolution of retreating subduction boundaries formed during continental collision. Tectonics 12 (3), 629–638.

Schellart, W.P., Moresi, L., 2013. A new driving mechanism for back-arc extension and backarc shortening through slab sinking induced toroidal and poloidal mantle flow: results from dynamic subduction models with an overriding plate. J. Geophys. Res. Solid Earth 118, 3221–3248. https://doi.org/10.1002/jgrb.50173.

Schmidt, C.J., Astini, R.A., Costa, C.H., Gardini, C.E., Kraemer, P.E., 1995. Cretaceous rifting, alluvial fan sedimentation, and Neogene inversion, southern Sierras Pampeanas. Argentina.

Sims, J.P., Ireland, T.R., Camacho, A., Lyons, P., Pieters, P.E., Skirrow, R.G., Stuart-Smith, P.G., Miró, R., 1998. U-Pb, Th-Pb and Ar-Ar geochronology from the southern Sierras Pampeanas, Argentina: implications for the Palaeozoic tectonic evolution of the western Gondwana margin. Geol. Soc. Spec. Publ. 142, 259–281. https://doi.org/10.1144/GSL.SP.1998.142.01.13.

Smith, P.M., Asimow, P.D., 2005. Adiabat_1ph: a new public front-end to the MELTS, pMELTS, and pHMELTS models. Geochem. Geophys. Geosyst. 6 https://doi.org/10.1029/2004GC000816.

Sobolev, A.V., Hofmann, A.W., Sobolev, S.V., Nikogosian, I.K., 2005. An olivine-free mantle source of Hawaiian shield basalts. Nature 434, 590–597. https://doi.org/10.1038/nature03411.

Sun, S.S., McDonough, W.F., 1989. Chemical and isotopic systematics of oceanic basalts: implications for mantle composition and processes. Geol. Soc. Spec. Publ. 42 (1), 313–345. https://doi.org/10.1144/GSL.SP.1989.042.01.19.

Thorkelson, D.J., Breitsprecher, K., 2005. Partial melting of slab window margins: genesis of adakitic and non-adakitic magmas. Lithos 79, 25–41. https://doi.org/10.1016/j.lithos.2004.04.049.

Till, C.B., Grove, T.L., Carlson, R.W., Donnelly-Nolan, J.M., Fouch, M.J., Wagner, L.S., Hart, W.K., 2013. Depth and temperatures of <10.5 Ma mantle melting and the lithosphere-asthenosphere boundary below southern Oregon and northern California. Geochem. Geophys. Geosyst. 14 (4), 864–879. https://doi.org/10.1002/ggge.20070.

Vergara, M., López-Escobar, L., Cancino, A., 1991. The Pichidangui Formation; Some geochemical characteristics and tectonic implications of the Triassic marine volcanism in central. Spec. Pap. Geol. Soc. Am. 265, 93. https://doi.org/10.1130/SPE265-p93.